Nature of the Displaceable Heme-Axial Residue in the *Ec*Dos Protein, a Heme-Based Sensor from *Escherichia coli*†

Gonzalo Gonzalez,‡ Elhadji M. Dioum,‡ Craig M. Bertolucci,‡ Takeshi Tomita,§ Masao Ikeda-Saito,|| Myles R. Cheesman,⊥ Nicholas J. Watmough,⊥ and Marie-Alda Gilles-Gonzalez*,‡

Departments of Biochemistry and Plant Biology and the Plant Biotechnology Center, The Ohio State University, 1060 Carmack Road, Columbus, Ohio 43210-1002, Institute of Multidisciplinary Research for Advanced Materials, Tohoku University, Katahira, Aoba, Sendai 980-8577, Japan, Department of Physiology and Biophysics, Case Western Reserve University School of Medicine, Cleveland, Ohio 44106-4970, and Schools of Biological and Chemical Sciences, University of East Anglia, Norwich NR4 7TJ, United Kingdom

Received March 20, 2002; Revised Manuscript Received May 7, 2002

ABSTRACT: The *Ec*Dos protein belongs to a group of heme-based sensors that detect their ligands with a heme-binding PAS domain. Among these various heme-PAS proteins, *Ec*Dos is unique in having its heme iron coordinated at both axial positions to residues of the protein. To achieve its high affinities for ligands, one of the axial heme-iron residues in *Ec*Dos must be readily displaceable. Here we present evidence from mutagenesis, ligand-binding measurements, and magnetic circular dichroism, resonance Raman, and electron paramagnetic resonance spectroscopies about the nature of the displaceable residue in the heme-PAS domain of *Ec*Dos, i.e., *Ec*DosH. The magnetic circular dichroism spectra in the near-infrared region establish histidine−methionine coordination in met-*Ec*Dos. To determine whether in deoxy-*Ec*Dos coordination of the sixth axial position is also to methionine, methionine 95 was substituted with isoleucine. This substitution caused the ferrous heme iron to change from an exclusively hexacoordinate low-spin form (*Ec*DosH) to an exclusively pentacoordinate high-spin form (M95I *Ec*DosH). This was accompanied by a modest acceleration of the dissociation rates of ligands but a dramatic increase (60−1300-fold) in the association rate constants for binding of O_2, CO, and NO. As a result, the affinity for O_2 was enhanced 10-fold in M95I *Ec*DosH, but the partition constant $M = [K_d(O_2)/K_d(CO)]$ between CO and O_2 was raised to about 30 from the extraordinarily low *Ec*DosH value of 1. Thus a major consequence of the increased O_2 affinity of this sensor was the loss of its unusually strong ligand discrimination.

In 1994 the term "heme-based sensors" was coined to describe a newly appreciated class of heme proteins that function in signal transduction (*1*). In these modular proteins the status of a heme cofactor bound to a heme-binding domain regulates the activity of a separate transducing domain. The prototypes for this broad functional class are the rhizobial FixL histidine protein kinases and the mammalian soluble guanylyl cyclases (*2*−*5*). This category of heme proteins has greatly expanded. It now includes DNA-binding proteins, such as the CooA protein of *Rhodospirullum rubrum* that regulates CO catabolism based on CO availability, and the chemotaxis methyl carrier proteins, such as the HemAT proteins of various Bacteria and Archaea that regulate movement toward O_2 (*6*−*10*). On the basis of protein sequence comparisons and known three-dimensional structures, regulatory hemes occur in a variety of protein structural folds. The most adaptable class of sensory hemes is held in an α-*β* three-dimensional fold called a PAS[1] fold (*11*). This fold is correlated with signal transduction but not exclusively associated with heme (*12*). Heme-PAS-containing proteins are involved in at least two major modes of signal transduction: control of phosphoryl transfer to regulatory proteins and control of cyclic nucleotide second messenger levels (*3*). The former group includes the FixL proteins of *Rhizobia* and the *Mt*Dos protein of *Methanobacterium thermoautotrophicum* (*1*, *2*, *13*). The *Sinorhizobium meliloti* and *Bradyrhizobium japonicum* FixL proteins control gene expression with an O_2-responsive histidine protein kinase activity (*14*−*16*). The latter group includes the PDEA1 protein of *Acetobacter xylinum* and the Dos protein of *Escherichia coli. Ax*PDEA1 governs the synthesis of a

† This research was supported by U.S. Public Health Service Grants HL-64038 and GM-57272 and by Grants-in-Aid (12480176 and 12147201) from the Ministry of Education, Science, Technology, Culture, and Sports, Japan.

* Corresponding author. Tel: (614) 688-3303. Fax: (614) 688-3302. E-mail: gilles-gonzalez.1@osu.edu, gilles.gonzalez@utsouthwestern.edu.

‡ The Ohio State University.

§ Tohoku University.

|| Case Western Reserve University School of Medicine.

⊥ University of East Anglia.

[1] Abbreviations: *Ec*Dos, *Escherichia coli* direct oxygen sensor; *Ec*DosH, *Ec*Dos heme-binding domain; PAS, sensory domain named after the eukaryotic proteins *P*eriod, *A*RNT, and *S*imple-minded; heme-PAS, heme-binding PAS; *Bj*FixLH, *Bradyrhizobium japonicum* FixL heme-binding domain; *Ax*PDEA1, *Acetobacter xylinum* phosphodiesterase A1; *Ax*PDEA1H, *AxPDEA1* heme-binding domain; EPR, electron paramagnetic resonance; MCD, magnetic circular dichroism; NIR-CT, near-infrared charge transfer; h, hexacoordinate heme iron with protein side chains as axial ligands; p, pentacoordinate heme iron; K_{hp}, equilibrium dissociation constant for the hexacoordinate-to-pentacoordinate transition; deoxy, having Fe^{II} without exogenously added ligand; met, having Fe^{III} without exogenously added ligand.

10.1021/bi025845x CCC: $22.00
Published on Web 06/07/2002

polysaccharide matrix with an O_2-responsive cyclic diGMP phosphodiesterase activity (*17*, *18*). *Ec*Dos shares more than 40% sequence identity with *Ax*PDEA1 over its heme-binding and enzymatic domains (*19*, *20*).

*Ec*Dos is unique among the known heme-PAS sensors in having its heme iron coordinated at both axial positions to protein residues (*13*, *20*). Exogenous ligands must readily displace one of the resident axial ligands from the heme iron, since ferrous *Ec*DosH binds O_2 and CO, and ferric *Ec*DosH binds CN^-, with high affinity (*20*). Such a side-chain displacement suggests a very direct mechanism for a ligand-induced protein conformational change. Although it is not yet clear to what extent the heme-iron coordination governs the ligand-binding behavior of *Ec*Dos, this behavior is already known to be highly unusual (*20*). For example, O_2 dissociates from *Ec*DosH at the very slow rate of 0.034 s^{-1}. This off-rate is much slower than the 5−20 s^{-1} value typical of hemoglobins and other heme-PAS proteins, although it falls within the range observed for some cereal hemoglobins having hexacoordinate heme iron (*21*, *22*). Unlike the plant hemoglobins, the association rate constant for binding of O_2 to *Ec*DosH is also extremely slow (0.0026 μM^{-1} s^{-1}) (*20*).

For displaceable-residue heme proteins, the ligand-binding parameters depend on the equilibrium between the fraction of protein in a pentacoordinate heme-iron conformation with an available ligand-binding site on the distal side and a hexacoordinate conformation without an available ligand-binding site. For *Ec*DosH, the observed rates of association with ligands increase linearly with respect to ligand concentration up to the maximum achievable concentrations, without approaching a limiting, concentration-independent, value (*20*). This linear behavior has at least two important implications. First, the off-rate of the displaceable residue must be much faster than the fastest measured on-rate for binding of a ligand to *Ec*DosH (~1.7 s^{-1} for O_2). Second, the equilibrium between the hexacoordinate and pentacoordinate conformations must be rapid compared to the rate of ligand association. This behavior is similar to that of rice hemoglobin but quite different from the example of barley hemoglobin (*21*, *22*). In barley hemoglobin, the off-rate of a displaceable axial histidine (~0.043 s^{-1}) limits the maximum achievable on-rate for ligands regardless of the ligands or their concentration (*21*). Here we combine mutagenesis and spectroscopic approaches to identify the displaceable residue in *Ec*Dos and determine how that residue influences sensing of heme ligands.

MATERIALS AND METHODS

Genetic Manipulation. A recombinant gene fragment corresponding to codons 1−147 of the *Ecdos* gene served as the template for site-directed mutagenesis by the polymerase chain reaction (*20*). Individual mutations were generated by the QuickChange site-directed mutagenesis protocol (Stratagene) and confirmed by sequencing of both strands of the DNA (Plant-Microbe Genomics Facility, The Ohio State University). The final constructs, containing *EcdosH* under control of the *tac* promoter on a plasmid conferring ampicillin resistance, were transformed into *E. coli* strain TG1 for expression.

Purification and Preparation of Proteins. Purification of *Ec*DosH proteins with and without individual amino acid substitutions was essentially as described for the unmodified *Ec*DosH (*20*). The protein was recovered predominantly in the oxy form. Deoxy-*Ec*DosH was prepared by reducing the heme with crystalline sodium dithionite and removing the sodium dithionite by gel filtration on a column (5 mL Sephadex G-25) preequilibrated with deoxygenated 0.1 M Tris-HCl, pH 8.0. Likewise, met-*Ec*DosH was prepared by oxidizing the heme with 1 molar equiv of potassium ferricyanide and removing the potassium ferricyanide by gel filtration. Homogeneously oxy- or carbonmonoxy-*Ec*DosH was prepared by equilibrating deoxy-*Ec*DosH with 1 atm of O_2 or CO, respectively. Unless otherwise noted, all purified proteins were in 0.1 M Tris-HCl, pH 8.0.

Spectroscopic Measurements. Absorption spectra were recorded for protein in stoppered quartz cuvettes, with 0.2 and 1 cm path lengths, on an ATI UV5 or a Hitachi U-4001 spectrophotometer. Raman scattering was excited with the 413.1 nm line of a krypton ion laser (Spectra Physics) or the 441.6 nm line of a He−Cd laser (Kinmon Electronics) and detected by a CCD camera attached to a single polychromator (Ritsu Oyokogaku, DG-1000), as previously described (*13*). Electron paramagnetic resonance spectra were recorded on a Brüker ESP-300 X-band spectrometer fitted with a liquid helium flow cryostat. Magnetic circular dichroism spectra were recorded on circular dichrographs, JASCO J-500D, for the wavelength range 280−1000 nm, and JASCO J-730 for the range 800−2000 nm (*23*). Samples were mounted in an Oxford Instruments SM1 6-tesla superconducting solenoid with an ambient temperature 25 mm bore for room temperature measurements.

Ligand Binding. All measurements of ligand binding were done at 25 °C with solutions of protein (4−8 μM) in 0.1 M Tris-HCl, pH 8.0, and 5 mM dithiothreitol, and solutions of ligand in 0.1 M Tris-HCl, pH 8.0. Rates of ligand association were measured with a stopped-flow spectrometer (Applied Photophysics Ltd., Leatherhead, U.K.) at a wavelength of maximum difference between the starting and final species. Specifically, for ferrous M95I *Ec*DosH the rates were followed from the change in absorbance at 436 nm for O_2, 424 nm for CO, and 438 nm for NO, after the protein was mixed with 80−410 μM O_2, 50−480 μM CO, or 90−470 μM NO, respectively. Cyanide saturation was followed at 428 nm for ferric M95I *Ec*DosH and at 412 nm for ferric *Ec*DosH. For each ligand concentration, the apparent rate of association was measured at least three times. Rate constants were calculated from linear plots of k_{obs} versus ligand concentration, each including at least four ligand concentrations. Rates of dissociation were measured by ligand displacement. Oxygen dissociation was measured by monitoring formation of carbonmonoxy protein at 424 nm after 500 μM CO was added to oxy-M95I *Ec*DosH equilibrated with 100 μM O_2. Carbon monoxide dissociation was measured by monitoring formation of NO-bound protein at 426 nm following addition of 500 μM NO to carbonmonoxy-M95I *Ec*DosH equilibrated with 20 μM CO. Cyanide dissociation was monitored after free cyanide was removed from cyanomet-*Ec*DosH by gel filtration (5 mL Sephadex G-25 column).

Laser Photolysis. Photolysis of carbonmonoxy-*Ec*DosH (1 μM) in CO-saturated 20 mM Tris-HCl, pH 8.0, was initiated with a pulse of laser light (6 ns, 100 mJ, 532 nm) provided by a SL282G Nd:YAG laser equipped with

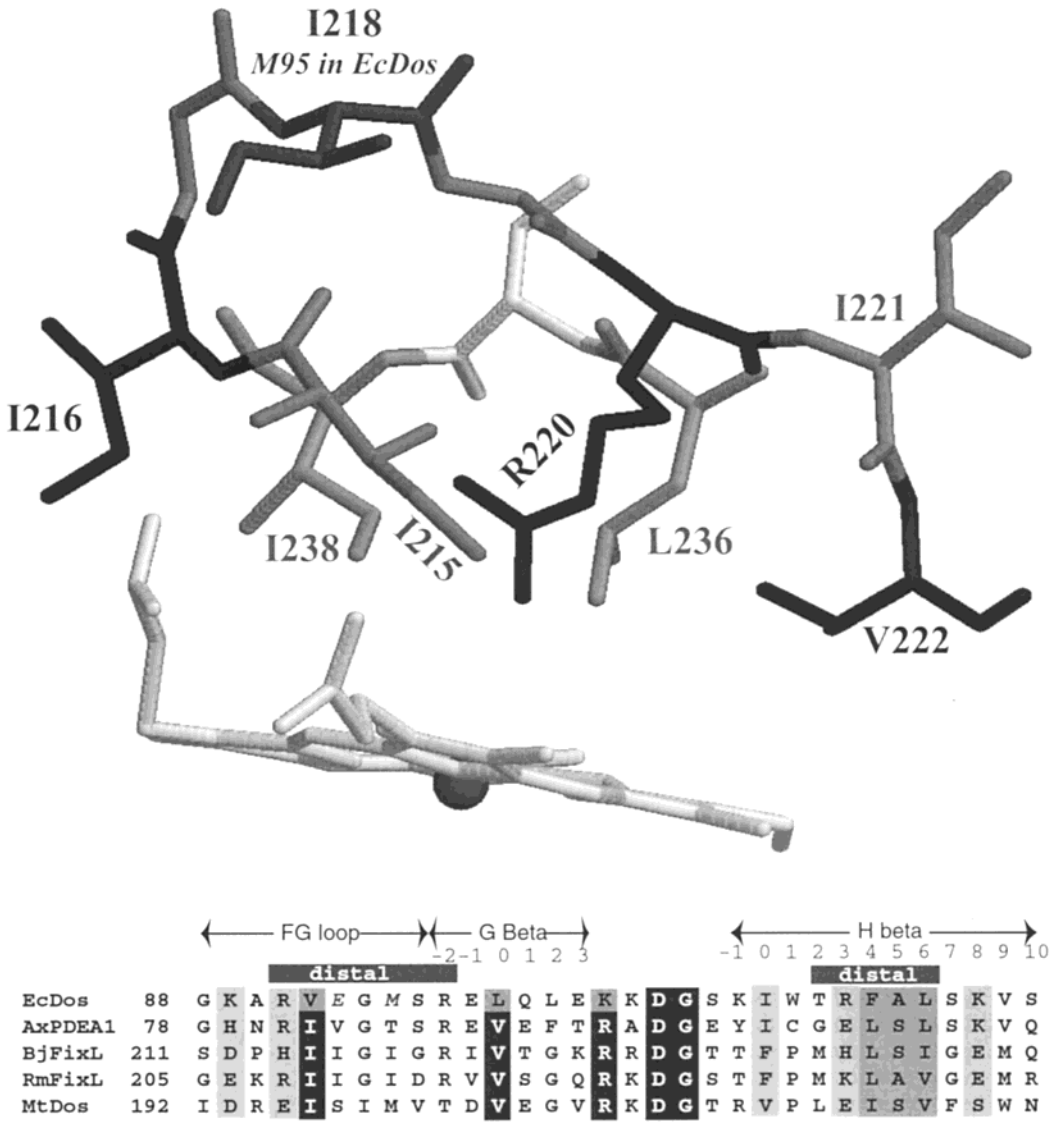

FIGURE 1: Heme pocket regions of heme-PAS proteins. The top part shows the structure of the heme distal pocket in met-*Bj*FixLH (*11*). The bottom part shows a secondary structure alignment for the heme distal pocket regions of *E. coli* Dos, *A. xylinum* PDEA1, *B. japonicum* FixL, *S. meliloti* FixL, and *M. thermoautotrophicum* Dos. Methionine 95 in *Ec*Dos is naturally replaced by an isoleucine in *Bj*FixL (Ile 218). Arginine 97 in *Ec*Dos is the well-conserved arginine $G_\beta-2$ also in *Bj*FixL (Arg 220).

frequency-doubling optics (Spectron Laser Systems, Rugby, U.K.). Subsequent absorption changes at a single wavelength (2.5 nm intervals) were recorded with a Hewlett-Packard 54520A digitizing oscilloscope. On the basis of the changes in absorbance at all wavelengths as a result of a flash and the known difference spectra of *Ec*DosH, approximately 80% of bound CO was photolyzed.

RESULTS AND DISCUSSION

Structure and Sequence of Heme-PAS Domains. From heme-PAS domains for which structures are known, the sequences of heme-PAS domains share considerable homology over the region lining the heme distal pocket. Only two residues in the presumed distal pocket of *Ec*Dos are theoretically capable of coordinating to heme iron. One is the highly conserved $G_\beta-2$ arginine (Arg 97) that could easily reach the heme iron, with very little distortion from a structure modeled on *Bj*FixLH (Figure 1). The other is a methionine in the FG loop (Met 95) that could not reach the heme iron unless the structure of the *Ec*Dos heme domain were substantially distorted from that of *Bj*FixLH.

A Methionine Is the Displaceable Residue in Met-EcDosH. The magnetic circular dichroism spectra of met-*Ec*DosH conclusively show histidine−methionine coordination for the ferric form of this protein (Figure 2). The band observed in the ~1920 nm region MCD of met-*Ec*DosH is associated with histidine−methionine coordination (Figure 2C). The exact energy of this porphyrin (π)-to-ferric (d) charge-transfer transition at near-infrared wavelengths for low-spin ferric hemes responds predictably and systematically to changes in axial ligation (*24*, *25*). This NIR-CT band usually appears as a positive band often with a vibrational sideband to lower energy. The small band in the 660−710 nm region MCD of met-*Ec*DosH in Figure 6B is also characteristic of low-intensity ligand-to-metal charge-transfer transitions that occur when low-spin ferric heme is coordinated to sulfur as in cytochrome *c* (from methionine), bacterioferritin (bismethionine), or cytochrome P450 (cysteinate) (*26*−*28*). The coordination of methionine to the *Ec*Dos heme iron implies a substan-

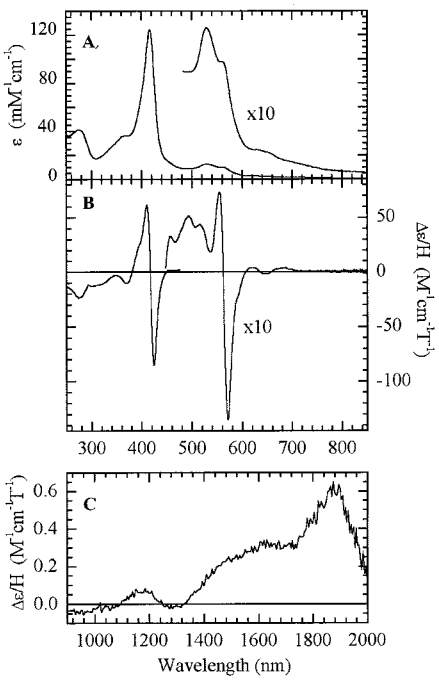

FIGURE 2: Absorption and magnetic circular dichroism spectra of met-*Ec*DosH. Absorption spectrum in the ultraviolet and visible regions (A), MCD spectrum in the ultraviolet and visible regions (B), and MCD spectrum in the near-infrared region (C) for met-*Ec*DosH at room temperature. The met-*Ec*DosH concentrations were 8 and 262 μM for the absorption and the MCD spectra, respectively. The MCD spectra were recorded with a magnetic field of 6 T.

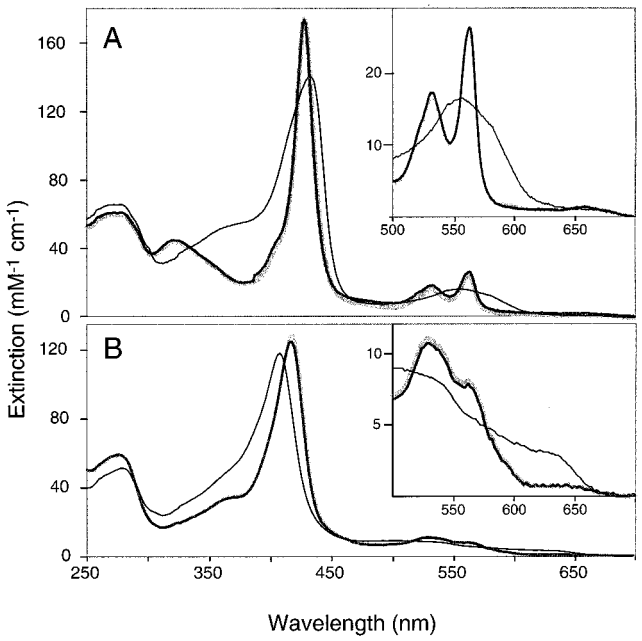

FIGURE 3: Influence of the M95I and R97A substitutions on the absorption spectra of *Ec*DosH. Part A shows the absorption spectra of the deoxy forms of M95I *Ec*DosH (thin line), R97A *Ec*DosH (gray line), and *Ec*DosH (thick line). Part B shows the absorption spectra of the met forms of M95I *Ec*DosH (thin line), R97A *Ec*DosH (gray line), and *Ec*DosH (thick line). All proteins were at 23 °C in 50 mM Tris-HCl, 50 mM NaCl, and 5% glycerol (v/v), pH 8.0. The spectra of *Ec*DosH and R97A *Ec*DosH are superimposed in each panel and are essentially identical.

tial reorganization of the *Ec*DosH heme distal pocket compared to the known heme-pocket structures of *Bj*FixLH and *Rm*FixLH. In these structures the residue corresponding to methionine 95 (Ile 218 in *Bj*FixLH, Ile 212 in *Rm*FixLH), based on sequence comparisons, points away from the heme pocket and is relatively far from the iron atom (Figure 1).

A Methionine at Position 95 Is the Displaceable Residue in Deoxy-EcDosH. The assignment of a methionine as the displaceable residue in ferric *Ec*DosH did not necessarily mean that methionine is also the displaceable residue in ferrous *Ec*DosH. Ferrous CooA protein, for example, has histidine coordination to the distal side, but the ferric form of this protein has cysteine coordination (*7*, *29*). To test whether ferrous *Ec*DosH heme iron is coordinated to methionine, we prepared an *Ec*DosH variant with an isoleucine replacing the only methionine in the heme distal pocket, i.e., methionine 95. UV−visible absorption and resonance Raman spectra confirmed that the heme iron in deoxy-M95I *Ec*Dos is pentacoordinate and high spin, in contrast to the heme iron in deoxy-*Ec*Dos, which is clearly hexacoordinate and low spin. Specifically, in the UV−visible spectra of deoxy-M95I *Ec*DosH a broad Soret peak at 434 nm and a very broad absorption band in the 500−600 nm region, indicative of pentacoordinate high-spin heme iron, replaced the characteristically sharp Soret peak at 427 nm and well-resolved β- and α-bands (532 and 563 nm, respectively) of the hexacoordinate low-spin deoxy-*Ec*Dos (Figure 3A). The resonance Raman characteristic modes ν_4 and ν_3, which are very sensitive to spin and electron density, also confirmed a predominantly pentacoodinate and low-spin heme iron in deoxy-M95I *Ec*DosH (ν_4 = 1362 and ν_3 = 1494 cm^{-1}), in contrast to the hexacoordinate high-spin heme iron in deoxy-*Ec*DosH (ν_4 = 1356 and ν_3 = 1472 cm^{-1}) (Figure 4A,B). Moreover, an Fe−His stretch was clearly visible at 213 cm^{-1} for the pentacoordinate deoxy-M95I *Ec*DosH (Figure 4F). As expected for the resonance Raman spectrum of protein having hexacoordinate low-spin heme iron, the Fe−His stretch was not observable for deoxy-*Ec*DosH (Figure 4E, Table 1). The simplest explanation for the effects on the spectra of *Ec*DosH of substituting isoleucine at position 95 is that methionine 95 is the displaceable residue. As a test of the possibility that introducing an isoleucine at position 95 might interfere with coordination of another residue, we examined the effect on coordination of substituting arginine 97 with alanine. This arginine is the only other residue in the *Ec*DosH distal pocket that could potentially coordinate to the heme iron (Figure 1). The absorption spectra of R97A *Ec*DosH were essentially identical to the corresponding spectra of *Ec*DosH, and all spectroscopic evidence was consistent with the heme iron of R97A *Ec*DosH being predominantly hexacoordinate in both the deoxy and met forms (Figure 3).

Spin and Coordination in Normal Ferric EcDosH. Resonance Raman, EPR, and MCD spectra of met-*Ec*DosH were consistent with this protein having predominantly hexacoordinate heme iron, with the majority of this hexacoordinate heme iron being low spin and a minor proportion (<10%) being high spin. The pentacoordinate fraction was below the detection limit of resonance Raman spectroscopy, which showed only the hexacoordinate and low-spin heme iron (ν_4 = 1370 and ν_3 = 1505 cm^{-1}) (Figure 4, Table 1). With EPR, high-spin as well as low-spin ferric heme iron was detectable, with the $g \sim 5.85$ feature indicating a

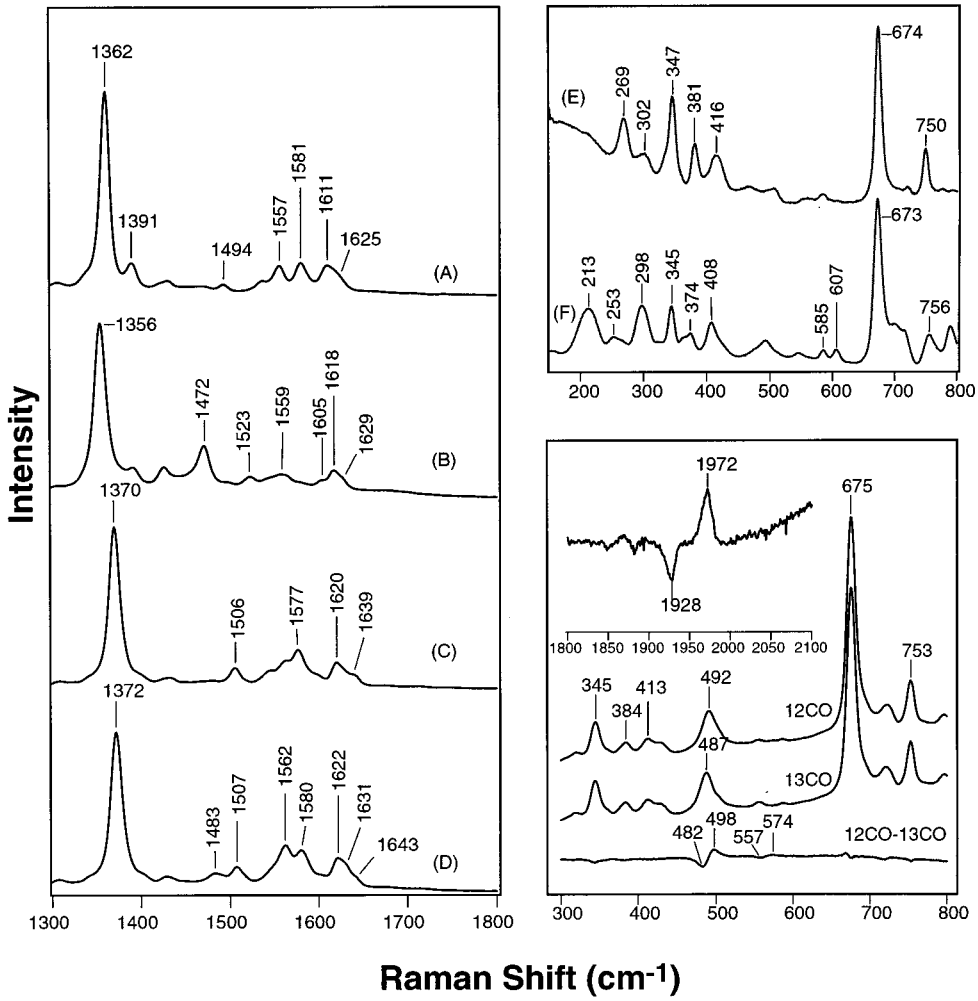

FIGURE 4: Comparison of the resonance Raman spectra of *Ec*DosH and M95I *Ec*DosH. The left panel shows the resonance Raman spectra of deoxy-*Ec*DosH (A), deoxy-M95I *Ec*DosH (B), met-*Ec*DosH (C), and met-M95I *Ec*DosH (D), obtained with 413.1 nm excitation. The top right panel shows spectra of the deoxy forms of *Ec*DosH (E) and M95I *Ec*DosH (F), obtained with 441.6 nm excitation. The bottom right panel shows spectra of carbonmonoxy-M95I *Ec*DosH obtained with 413.1 nm excitation. Relevant vibrational frequencies from this figure are tabulated in Tables 1 and 3.

Table 1: Raman Frequencies of Porphyrin Skeletal Modes for Normal and M95I *Ec*DosH

	coordination[a]	ν_4[b]	ν_3	ν_2	ν_{10}	ν_{Fe-His}
oxidized (met, Fe^{III})						
*Ec*DosH	6-c LS	1370	1506	1577	1639	
M95I *Ec*DosH	6-c HS/6-c LS	1372	1483/1507	1580/1562	1631/1643	
reduced (deoxy, Fe^{II})						
EcDosH	6-c LS	1362	1494	1581	1625	nd[c]
M95I *Ec*DosH	5-c HS	1356	1472	1559	1605	213

[a] Heme-iron coordination: 5-c, pentacoordinate; 6-c, hexacoordinate; HS, high spin; LS, low spin. [b] All frequencies are in units of cm^{-1}. [c] Not detected.

relatively small proportion of high-spin ferric heme iron and the $g = 3.42$ feature indicating a high proportion of low-spin ferric heme iron (Figure 5). The asymmetry of the $g = 3.42$ feature is typical of "large g_{max}"-type spectra. The majority of such species give rise to "rhombic" EPR spectra with three observable features. However, if the axial-ligand orientation imposes relatively high symmetry at the ferric iron, then the d_{xz},d_{yz} orbitals are nearly degenerate, and the unpaired electron is significantly delocalized between them. Consequently, the g_z feature moves to lower field, and g_x and g_y are often broad and undetectable (*30*). The MCD spectra of met-*Ec*DosH support those results (*24*, *31*) (Figure 6C). The 300−600 nm region was very characteristic of low-spin ferric heme in both form and intensity (Figure 6). On the other hand, the weak derivative feature at 600−660 nm indicated a charge-transfer band and signaled the presence of a small population (<10%) of high-spin ferric heme iron having histidine and water as the axial ligands (*32*, *33*).

Spin and Coordination in Ferric M95I EcDosH. The absorption spectrum of met-M95I *Ec*DosH was myoglobin-like and typical of ferric heme proteins having high-spin water-coordinated heme iron (Figure 3B). Specifically, the spectrum of met-M95I *Ec*DosH featured a Soret band at 408 nm, a broad peak in the 475−575 nm region, and a small charge-transfer band in the 625−675 nm region. From the resonance Raman spectra of met-M95I *Ec*DosH, it was clear

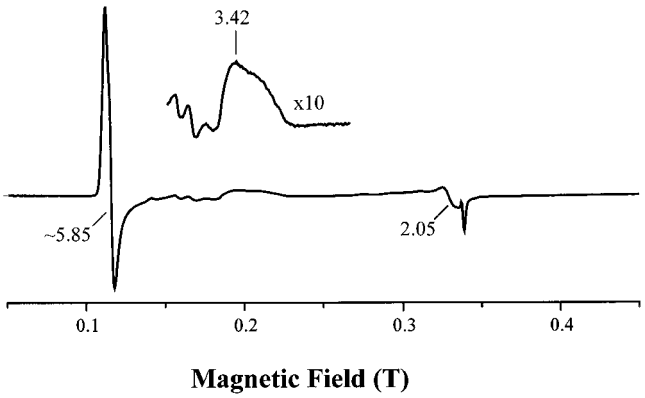

FIGURE 5: X-band EPR spectra of met-*Ec*DosH. The apparent *g*-values of features discussed in the text are labeled. The low-spin feature ($g = 3.42$) is expanded in the inset. Conditions: sample concentration, 2 mM met-*Ec*DosH; temperature, 8 K; microwave power, 1 mW; modulation amplitude, 10.1 G.

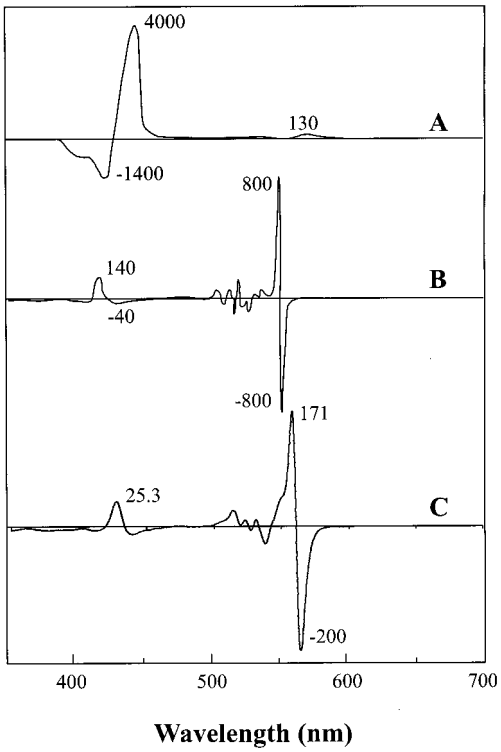

FIGURE 6: Magnetic circular dichroism spectrum of deoxy-*Ec*DosH. Room temperature MCD spectra of high-spin deoxymyoglobin (A), low-spin ferrocytochrome *c* (B), and deoxy-*Ec*DosH (C). The intensities, in units of M^{-1} cm^{-1} T^{-1}, are noted at the prominent peak and trough wavelengths. The deoxy-*Ec*DosH spectrum was recorded with 262 μM protein and a magnetic field of 6 T. The sharp derivative for *Ec*DosH near 560 nm with small oscillations to higher energy is absolutely typical for low-spin ferrous heme. Though these bands do vary in intensity, the 400 M^{-1} cm^{-1} T^{-1} peak-to-trough intensity in (C) could easily account for all of the heme present. The data in (A) and (B) are from Cheesman et al. (*26*).

that the ferric heme iron remained hexacoordinate but became a mixture of high and low spin (Figure 4C,D). Compared to the ν_3 mode of met-*Ec*DosH at 1506 cm^{-1}, the ν_3 of met-M95I *Ec*DosH was noticeably split into two modes occurring at 1483 and 1507 cm^{-1}. A mixture of ligation to water (a high-spin ligand) and hydroxide (a mixed-spin ligand) would account for the observed absorption and resonance Raman

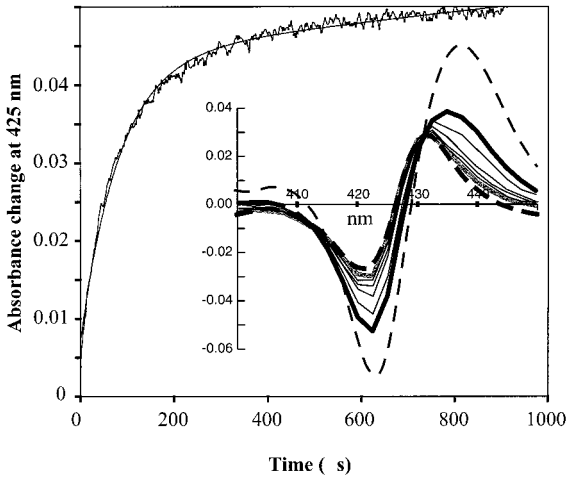

FIGURE 7: Association rate of the displaceable methionine in ferrous *Ec*DosH. Time course of absorbance at 425 nm following photolysis of 10 μM carbonmonoxy-*Ec*DosH, in CO-saturated buffer, with a 6 ns, 100 mJ pulse from a Nd:YAG laser. The dominant rate is 12000 s^{-1}. The inset shows the absorption spectra of existing species minus the spectrum of the starting carbonmonoxy form. The first spectrum shown was recorded 49 μs following photolysis of the CO (thick black line); the final spectrum shown was collected 879 μs after the photolysis (thick gray line). The CO difference spectra of deoxy-M95I EcDosH (thin dotted line) and deoxy-*Ec*DosH (thick dotted line) are provided as the standards for the transition from pentacoordinate deoxy to hexacoordinate deoxy, respectively.

spectra, and the effect of pH on those spectra is consistent with this interpretation (data not shown).

The Association Rate of the Displaceable Methionine and Its Implications. About 80% pentacoordinate (p-state) deoxy-*Ec*DosH can be produced essentially instantaneously by photodissociating CO from carbonmonoxy-*Ec*DosH with a laser. Since the rate of association of the methionine to the heme iron is expected to be much faster than the rate of rebinding of CO, rebinding of the methionine should dominate the early phase of relaxation. The end product of this first phase of reaction is the hexacoordinate (h-state) deoxy-*Ec*DosH. In the second phase of the reaction, CO displaces the methionine, restoring the original equilibrium state of carbonmonoxy-*Ec*DosH. Since the absorption spectra of the hexacoordinate deoxy-*Ec*DosH and carbonmonoxy-*Ec*DosH are known, the two processes (methionine binding, then CO binding) can be easily distinguished from the spectra of the product species. Figure 7 shows the time course of absorbance at 425 nm following photolysis of carbonmonoxy-*Ec*DosH with a pulse from a Nd:YAG laser. During the first 100 μs after the laser pulse, the change in absorbance at 425 nm was independent of the CO concentration and dominated by a 12000 s^{-1} process. The observed difference spectra from 400 to 450 nm showed this process to be a transition from the pentacoordinate to the hexacoordinate form (Figure 7, inset).

Some Predictions for Binding of Exogenous Ligands to a Displaceable-Residue Heme Protein. If the association of an external ligand with the *Ec*Dos heme iron is regarded simply as a competitive displacement of methionine 95 by the ligand, then the observed rate of binding of the ligand L will have the form $R = (k_{hp}L'' + k_{ph})/(k_{ph} + l'')$. In this equation k_{ph} is the rate of going from the p- to h-state or the association rate of methionine 95, k_{hp} is the rate of going from the h- to p-state or the dissociation rate of methionine

Table 2: Influence of the M95I Substitution on the Ligand-Binding Parameters of *Ec*DosH at 25 °C

	O_2			CO			NO	CN^-	
	k_{on} ($\mu M^{-1}\,s^{-1}$)	k_{off} (s^{-1})	K_d (μM)	k_{on} ($\mu M^{-1}\,s^{-1}$)	k_{off} (s^{-1})	K_d (μM)	k_{on} ($\mu M^{-1}\,s^{-1}$)	k_{on} ($mM^{-1}\,s^{-1}$)	k_{off} (s^{-1})
M95I *Ec*DosH	0.16	0.22	1.4[a]	1.1	0.05	0.05[a]	2.4	0.071	3.8×10^{-5}
*Ec*DosH[b]	0.0026	0.034	13	0.0011	0.011	10	0.0018	0.014	6.2×10^{-5}
*Ax*PDEA1H[c]	6.7	77	12	0.021	0.0058	0.27		0.27	1.5×10^{-4}

[a] Calculated from the corresponding k_{off}/k_{on}. [b] Delgado-Nixon et al. (*20*). [c] Chang et al. (*18*).

95, L'' is the ligand concentration multiplied by the rate constant for association of the ligand to the p-state, and l'' is the rate of dissociation of the ligand from *Ec*DosH. Thus the observed approach to equilibrium is not generally linear with respect to ligand concentration. There are two simplified cases for competitive displacement of the methionine by an external ligand L.

Case 1: If $l'' \ll k_{ph}$, then $R = L + (k_{hp}/k_{ph})L'[L] = L + (k_{hp}L')[L]$. The observed rates are linear with respect to ligand concentration, and the slope gives the association rate of *Ec*Dos.

Case 2: If $Lk_{ph} \ll k_{hp}L'[L]$, then $1/R = 1/k_{hp} + [(k_{ph}/k_{hp})L'][L] = 1/k_{hp} + (L'/K_{hp})(1/[L])$. At high ligand concentrations, the observed rate is equal to k_{hp}, the dissociation rate of methionine 95.

The fast rate measured for k_{ph}, the spectroscopic evidence showing that a very high proportion of deoxy-*Ec*DosH is in the h-state, and the linearity of the on-rates with respect to ligand concentrations (up to the solubility limit of the ligands) all suggest that case 1 applies to *Ec*DosH. This would predict that for any ligand the association rate will simply be a constant (K_{hp}) times the rate that it would have if we could keep all the deoxy-*Ec*DosH permanently in the p-state. The presence of a displaceable residue in competition with the ligand should not affect the dissociation rate but should reduce the affinity for all ligands by a factor K_{hp}. It must be noted that in the case of some plant hemoglobins that have bishistidine-coordinated heme iron, substitution of the displaceable histidine causes a very large decrease, rather than an increase, in the affinities for polar ligands (*34*). This is because of the dual role of the distal histidine in those proteins. Unlike the distal methionine of *Ec*Dos, the distal histidine of plant hemoglobins also stabilizes the bound ligand that displaced it from the heme iron, and this stabilization more than compensates for competition of the histidine with the ligand.

*Effects of Methionine Coordination on the Ligand-Binding Properties of EcDos*H. Given that isoleucine is similar in size and polarity to methionine, if the location of the isoleucine is also similar to that of methionine 95 in the p-state, then deoxy-M95I *Ec*DosH could represent a fair approximation of the p-state of deoxy-*Ec*DosH. Since methionine is not expected to stabilize or destabilize directly any external ligands, the effect of the displaceable methionine on ligand binding should be limited to its role as a competitor. A true p-state *Ec*DosH would accelerate the association of all ligands of ferrous heme by the same factor, K_{hp}, but comparison of the on-rate constants for binding of ligands to deoxy-M95I *Ec*DosH versus deoxy-*Ec*DosH shows the extent of acceleration to be extremely ligand-dependent (Table 2). For example, compared to *Ec*DosH the association rate constant of M95I *Ec*DosH increased more than 1300 times for binding to NO, about 1000-fold for binding to CO, 60-fold for binding to O_2, and only 3-fold for binding of CN^-. The substitution had little effect on binding of O_2 (60-fold increase) and CN^- (3-fold increase) but a profound effect on binding of the less polar ligands NO (1300-fold increase) and CO (1000-fold increase). It is interesting to note that the C−O (1972 cm^{-1}) and Fe−CO (492 cm^{-1}) stretches of M95I *Ec*DosH were slightly higher than those of *Ec*DosH (1969 and 487 cm^{-1}, respectively), implying a changed geometry for the bound CO (Figure 4, Table 3). Those frequencies were also consistent with the bound CO having no electrostatic interaction with side chains of the protein on the distal side. Thus the isoleucine substitution at position 95 appears not to have introduced any major structural changes in the heme pocket (*13*).

Table 3: Resonance Raman Frequencies of Carbonmonoxy-M95I *Ec*DosH

protein	ν_{Fe-CO}[a]	ν_{C-O}	δ_{Fe-C-O}
M95I *Ec*DosH	492	1972	574
*Ec*DosH	487	1969	575

[a] All frequencies are in units of cm^{-1}.

The displaceable methionine appears important for adjusting the relative affinities of ligands, i.e., "ligand discrimination". For example, the replacement of methionine 95 with isoleucine caused the M value [$M = K_d(O_2)/K_d(CO)$] to rise from ~1 to 28, abolishing the extraordinarily high discrimination against CO previously noted for *Ec*DosH (*20*). A startling consequence of the extremely ligand-dependent acceleration of association in M95I *Ec*DosH is that CO binds 7 times more rapidly than O_2 to this protein (Table 2). Typically, CO binds to heme proteins 10−30 times more slowly than does O_2. It is this peculiarity of M95I *Ec*DosH that makes it feasible to measure O_2 off-rates by displacement with CO. To our knowledge, the only other heme protein, natural or engineered, to which CO binds faster than O_2 is *Ascaris* Hb (*35*). Interestingly, the O_2 affinity of M95I *Ec*DosH ($K_d \sim 1.4\ \mu M$) represents the highest O_2 affinity so far observed for a heme-PAS. Thus the relatively low affinities of most O_2 sensors of this class are not due to any intrinsic limitations of a heme-PAS fold. It is likely that physiological systems cover a quite broad range of affinities and discrimination with this type of fold.

The most mundane explanation for the strong ligand dependence of the acceleration of binding is that methionine is unbranched but isoleucine has a methyl group on its β-carbon. That methyl group might, either directly or indirectly by repositioning other side chains, stabilize a bound ligand relative to a protein with methionine in the equivalent displaced position. In such a case, the affinity of M95I *Ec*DosH for that ligand would increase more dramatically

than predicted from the loss of competition with methionine 95 alone. Another more interesting explanation invokes protein dynamics. Figure 7 suggests that a spontaneously generated p-state deoxy-*Ec*DosH has an average lifetime of less than 80 μs. Thus ligands binding to the "permanent p-state", caused by substituting methionine 95, encounter a fully equilibrated protein that has had unlimited time to adjust to the absence of methionine coordination, rather than the 80 μs allowed to natural p-state protein. Suppose the sensory conformational change that follows the displacement of the methionine from the *Ec*Dos heme iron, either by spontaneous dissociation or exogenous ligand displacement, takes longer than 80 μs. Then the permanent p-state of deoxy-M95I *Ec*DosH could be very different in its reactivity from the transient p-state resulting from the normal h ↔ p equilibrium.

A latent period in the sensory conformational change in *Ec*Dos comparable to the lifetime of a ligand-bound state could serve a purpose. Without a latent period, the *Ec*Dos sensor would "chatter" continuously between on- and off-states, in the absence of external ligand, as the displaceable methionine spontaneously associated and dissociated. With a latent period, *Ec*Dos would only switch to an off-state if the heme iron remained bound to an external ligand for longer than 80 μs. This feature would be analogous to the "debouncing" delay circuit in computer keyboards, which causes a refractory period after each key stroke and prevents a single key stroke from generating multiple characters due to bouncing of the keys. A latent period between binding of a ligand and completion of a conformational change could also exist for other sensing mechanisms, such as those of FixL proteins, that do not involve a displaceable residue.

REFERENCES

1. Gilles-Gonzalez, M. A., Gonzalez, G., Perutz, M. F., Kiger, L., Marden, M. C., and Poyart, C. (1994) *Biochemistry 33*, 8067−8073.
2. Gilles-Gonzalez, M. A., Ditta, G. S., and Helinski, D. R. (1991) *Nature 350*, 170−172.
3. Gilles-Gonzalez, M. A. (2001) Oxygen signal transduction, *IUBMB Life 51*, 165−173.
4. Craven, P. A., and DeRubertis, F. R. (1978) *J. Biol. Chem. 253*, 8433−8443.
5. Denninger, J. W., and Marletta, M. A. (1999) *Biochim. Biophys. Acta 1411*, 334−350.
6. Shelver, D., Kerby, R. L., He, Y., and Roberts, G. P. (1997) *Proc. Natl. Acad. Sci. U.S.A. 94*, 11216−11220.
7. Roberts, G. P., Thorsteinsson, M. V., Kerby, R. L., Lanzilotta, W. N., and Poulos, T. (2001) *Prog. Nucleic Acid Res. Mol. Biol. 67*, 35−63.
8. Hou, S., Larsen, R. W., Boudko, D., Riley, C. W., Karatan, E., Zimmer, M., Ordal, G. W., and Alam, M. (2000) *Nature 403*, 540−544.
9. Hou, S., Freitas, T., Larsen, R. W., Piatibratov, M., Sivozhelezov, V., Yamamoto, A., Meleshkevitch, E. A., Zimmer, M., Ordal, G. W., and Alam, M. (2001) *Proc. Natl. Acad. Sci. U.S.A. 98*, 9353−9358.
10. Hou, S., Belisle, C., Lam, S., Piatibratov, M., Sivozhelezov, V., Takami, H., and Alam, M. (2001) *Extremophiles 5*, 351−354.
11. Gong, W., Hao, B., Mansy, S. S., Gonzalez, G., Gilles-Gonzalez, M. A., and Chan, M. K. (1998) *Proc. Natl. Acad. Sci. U.S.A. 95*, 15177−15182.
12. Taylor, B. L., and Zhulin, I. B. (1999) *Microbiol. Mol. Biol. Rev. 63*, 479−506.
13. Tomita, T., Gonzalo, G., Chang, A. L., Ikeda-Saito, M., and Gilles-Gonzalez, M.-A. (2002) *Biochemistry 41*, 4819−4826.
14. Gilles-Gonzalez, M. A., and Gonzalez, G. (1993) *J. Biol. Chem. 268*, 16293−16297.
15. Tuckerman, J. R., Gonzalo, G., and Gilles-Gonzalez, M. A. (2001) *J. Mol. Biol. 308*, 449−455.
16. Lois, A. F., Weinstein, M., Ditta, G. S., and Helinski, D. R. (1993) *J. Biol. Chem. 268*, 4370−4375.
17. Ross, P., Mayer, R., and Benziman, M. (1991) *Microbiol. Rev. 55*, 35−58.
18. Chang, A. L., Tuckerman, J. R., Gonzalez, G., Mayer, R., Weinhouse, H., Volman, G., Amikam, D., Benziman, M., and Gilles-Gonzalez, M. A. (2001) *Biochemistry 40*, 3420−3426.
19. Tal, R., Wong, H. C., Clahoon, R., Gelfand, D., Fear, A. L., Volman, G., Mayer, R., Ross, P., Amikam, D., Weinhouse, H., Cohen, A., Sapir, S., Ohana, P., and Benziman, M. (1998) *J. Bacteriol. 180*, 4416−4425.
20. Delgado-Nixon, V. M., Gonzalez, G., and Gilles-Gonzalez, M. A. (2000) *Biochemistry 39*, 2685−2691.
21. Duff, S. M., Wittenberg, J. B., and Hill, R. D. (1997) *J. Biol. Chem. 272*, 16746−16752.
22. Arredondo-Peter, R., Hargrove, M. S., Sarath, G., Moran, J. F., Lohrman, J., Olson, J. S., and Klucas, R. V. (1997) *Plant Physiol. 115*, 1259−1266.
23. Thomson, A. J., Cheesman, M. R., and George, S. J. (1993) *Methods Enzymol. 226*, 199−232.
24. Cheesman, M. R., Greenwood, C., and Thomson, A. J. (1991) *Adv. Inorg. Chem. 36*, 201−255.
25. Gadsby, P. M. A., and Thomson, A. J. (1990) *J. Am. Chem. Soc. 112*, 5003−5011.
26. Moore, G. R., and Pettigrew, W. G. (1990) *Cytochromes c. Evolutionary, structural and physiochemical aspects*, Springer, Berlin.
27. Cheesman, M. R., Kadir, F. H. A., Al-Basseet, J., Al-Massad, F., Farrar, J., Greenwood, C., Thomson, A. J., and Moore, G. R. (1992) *Biochem. J. 286*, 361−367.
28. McKnight, J., Cheesman, M. R., Thomson, A. J., Miles, J. S., and Munro, A. W. (1993) *Eur. J. Biochem. 213*, 683−687.
29. Aono, S., Ohkubo, K., Matsuo, T., and Nakajima, H. (1998) *J. Biol. Chem. 273*, 25757−25764.
30. Walker, F. A. (1999) *Coord. Chem. Rev. 185−186*, 471−534.
31. Vickery, L., Salmon, A., and Sauer, K. (1975) *Biochim. Biophys. Acta 386*, 87−98.
32. Brill, A. S., and Williams, R. J. P. (1961) *Biochem. J. 78*, 246−253.
33. Braterman, P. S., Davies, R. C., and Williams, R. J. P. (1964) *Adv. Chem. Phys. 7*, 359−407.
34. Hargrove, M. S., Brucker, E. A., Stec, B., Sarath, G., Arredondo-Peter, R., Klucas, R. V., Olson, J. S., and Phillips, G. N., Jr. (2000) *Structure 8*, 1005−1014.
35. De Baere, I., Perutz, M. F., Kiger, L., Marden, M. C., and Poyart, C. (1994) *Proc. Natl Acad. Sci. U.S.A. 91*, 1594−1597.

BI025845X